THE JOURNAL OF BIOLOGICAL CHEMISTRY VOL. 290, NO. 1, pp. 272–283, January 2, 2015

Pivotal Role of Extended Linker 2 in the Activation of Gα by G Protein-coupled Receptor*

Received for publication, August 30, 2014, and in revised form, November 18, 2014 Published, JBC Papers in Press, November 20, 2014, DOI 10.1074/jbc.M114.608661

Jianyun Huang[1], **Yutong Sun**[1,2], **J. Jillian Zhang, and Xin-Yun Huang**[3]

From the Department of Physiology, Cornell University Weill Medical College, New York, New York 10065

Background: G protein-coupled receptors mainly signal through heterotrimeric G-proteins.
Results: We have demonstrated that mutations in the extended Linker 2 impaired the activation of $G\alpha_s$ by β-adrenergic receptors.
Conclusion: We have proposed a potential novel conduit from β-adrenergic receptors to the helical domain of $G\alpha_s$ subunit via the extended Linker 2.
Significance: Our systematic mutagenesis studies provide insights into the activation mechanism of G-proteins by receptors.

G protein-coupled receptors (GPCRs) relay extracellular signals mainly to heterotrimeric G-proteins (Gαβγ) and they are the most successful drug targets. The mechanisms of G-protein activation by GPCRs are not well understood. Previous studies have revealed a signal relay route from a GPCR via the C-terminal α5-helix of Gα to the guanine nucleotide-binding pocket. Recent structural and biophysical studies uncover a role for the opening or rotating of the α-helical domain of Gα during the activation of Gα by a GPCR. Here we show that β-adrenergic receptors activate eight $G\alpha_s$ mutant proteins (from a screen of 66 $G\alpha_s$ mutants) that are unable to bind Gβγ subunits in cells. Five of these eight mutants are in the αF/Linker 2/β2 hinge region (extended Linker 2) that connects the Ras-like GTPase domain and the α-helical domain of $G\alpha_s$. This extended Linker 2 is the target site of a natural product inhibitor of G_q. Our data show that the extended Linker 2 is critical for Gα activation by GPCRs. We propose that a GPCR via its intracellular loop 2 directly interacts with the β_2/β_3 loop of Gα to communicate to Linker 2, resulting in the opening and closing of the α-helical domain and the release of GDP during G-protein activation.

A structurally diverse repertoire of ligands, from photons to many hormones and neurotransmitters, activate G protein-coupled receptors (GPCRs)[4] to elicit their physiological functions (1, 2). GPCRs comprise a large and diverse superfamily, and family members have been identified in organisms as evolutionarily distant as yeast and human. Heterotrimeric G-proteins (Gαβγ) directly relay the signals from GPCRs (3–5). These G-proteins are composed of α, β, and γ subunits. The β and γ subunits are tightly associated and can be regarded as one functional unit. G-proteins function as molecular binary switches with their biological activity determined by the bound nucleotide (3–5). Upon ligand-binding, GPCRs increase the exchange of GDP bound on the Gα subunit with GTP, in the presence of Gβγ subunits. This leads to the dissociation of the Gα subunit from the Gβγ dimer resulting in two functional subunits (Gα and Gβγ). Both Gα and Gβγ subunits signal to various cellular pathways.

Over the past 30 years, great progress has been made in understanding the mechanisms by which heterotrimeric G-proteins regulate their downstream targets (6, 7). Recently a series of crystal structures of GPCRs in the inactive and active states, bound with antagonists, inverse agonists, or agonists, have elucidated the structural basis for the modulation and activation of GPCRs by ligands (1, 8, 9). A crystal structure of the complex of β_2-adrenergic receptor and G_s has revealed the structural changes in β_2-adrenergic receptor and G_s, the interacting regions, and residues between a GPCR and a G-protein (10). However, the molecular mechanisms by which GPCRs activate G-proteins are still not completely understood (11, 12).

The structure of Gα subunits consists of two domains: a Ras-like GTPase domain and an α-helical domain (6) (Fig. 1, *A* and *B*). These two domains are linked by Linker 1 and Linker 2 (Fig. 1*B*). Between these two domains lies a deep cleft within which GDP or GTP is tightly bound (Fig. 1, *A* and *B*). The nucleotide is essentially occluded from the bulk solvent, leading to a proposal that the helical domain is the inhibitory barrier and provides the regulatory entry point by GPCRs or Gβγ subunits (13–16).

One of the major remaining problems in the biology of GPCR/G-protein signaling is to experimentally demonstrate whether GPCRs or Gβγ subunits play the catalytic exchange role in Gα protein activation (17). In theory, the question could be straightforwardly answered with purified proteins of GPCRs, Gα and Gβγ subunits. However, purified GPCRs had no guanine-nucleotide exchange effect on Gα in the absence of Gβγ subunits (18, 19). A GPCR could only activate Gα in the presence of Gβγ (18, 19), leading some to believe that GPCRs were not the real catalysts, although they were required to initiate the activation event from agonist binding. Yet, purified Gβγ subunits alone also could not accelerate the guanine nucleotide exchange on Gα subunits (3, 20). In fact, Gβγ subunits inhibit the basal nucleotide exchange activity of Gα sub-

* This work was supported, in whole or in part, by National Institutes of Health Grant HL 91525 (to X.-Y. H.).
[1] Both authors contributed equally to this work.
[2] Present address: Dept. of Molecular and Cellular Oncology, The University of Texas, MD Anderson Cancer Center, Houston, TX 77030.
[3] To whom correspondence should be addressed. Tel.: 212-746-6362; Fax: 212-746-8690; E-mail: xyhuang@med.cornell.edu.
[4] The abbreviations used are: GPCR, G protein-coupled receptor; DM, dodecyl-β-D-maltoside; MEF, mouse embryonic fibroblast; β-AR, β-adrenergic receptor; GEF, guanine-nucleotide exchange factor.

units and behave as a guanine-nucleotide dissociation inhibitor (20). When the structure of Gβ was revealed to be similar to RCC1, a guanine-nucleotide exchange factor for the small GTPase Ran, Gβγ was proposed to be the real guanine-nucleotide exchange factor for Gα, whereas GPCRs served as a trigger (15, 21). Therefore, it remains a fundamental unsolved question: which one, a GPCR and/or Gβγ subunit, has the ability to catalyze the nucleotide exchange on Gα.

We reasoned that if GPCRs or Gβγ subunits are the nucleotide exchangers, we should be able to find mutants of GPCRs or Gβγ subunits that would accelerate the nucleotide exchange on Gα subunits in the absence of Gβγ or GPCRs, respectively. Alternatively, we might be able to find mutant Gα subunits that could be activated by GPCRs alone or by Gβγ alone. Here we describe our finding of a direct activation of some $G\alpha_s$ mutant proteins by β-adrenergic receptors without Gβγ subunits. Although our data do not exclude a possible additional catalytic role for Gβγ, it clearly demonstrates that GPCRs by themselves have the catalytic ability to activate Gα subunits. Furthermore, from this systematic study, a pivotal role for the αF/Linker 2/β2 region (extended Linker 2) in Gα activation has been uncovered. Therefore, we propose that the opening and closing of the two domains (the Ras-like GTPase domain and the helical domain) with Linker 2 as a pivot provide one of the mechanisms for Gα activation by GPCRs.

EXPERIMENTAL PROCEDURES

G-protein Purification—$G\alpha_s$ wild-type and mutant proteins were purified from *Escherichia coli*. The pGEX-6P-$G\alpha_s$ plasmid was transformed into bacteria strain BL21(DE3). One liter of bacterial culture was grown at room temperature until the absorbance at 600 nm was ~1. G-protein expression was induced with 0.5 mM isopropyl 1-thio-β-D-galactopyranoside for 18 h at room temperature. The bacterial pellet was resuspended in lysis buffer (50 mM Tris, pH 8.0, 150 mM NaCl, 1% Triton X-100, 0.1 mg/ml of lysozyme, and 0.2 mM PMSF) and incubated on ice for 30 min. After sonication, the lysate was spun down at 10,000 × *g* for 120 min at 4 °C. Glutathione-agarose resin (0.5 ml, from Sigma) was added to the supernatant after pre-equilibration of the resin with lysis buffer. The mixture was gently agitated at 4 °C for 3 h. After washing 3 times with 10 ml of washing buffer (50 mM Tris, pH 8.0, 100 mM NaCl, and 0.2 mM PMSF), GST-tagged $G\alpha_s$ proteins were eluted with 0.5 ml of elution buffer (50 mM Tris, pH 8.0, 100 mM NaCl, 1 mM EDTA, 1 mM DTT, and 10% glycerol). preScission protease (Amersham Biosciences) was used to cleave GST off at 4 °C overnight.

Gβγ Proteins Were Purified from Insect Hi5 Cells—One liter of Hi5 cell pellet was resuspended into 50 ml of lysis buffer (50 mM Tris, pH 8.0, 1 mM EDTA, and protease inhibitors: 10 μg/ml of leupeptin, 1 μg/ml of pepstatin A, 1 mM benzamidine, and 0.2 mM PMSF). After sonication, the lysate was spun down at 150,000 × *g* for 90 min at 4 °C. The membrane pellet was resuspended in 50 ml of lysis buffer. After homogenization, the lysate was centrifuged again. The final pellet was resuspended in 50 ml of extraction buffer (50 mM Tris, pH 8.0, 150 mM NaCl, 2% dodecyl-β-D-maltoside (DM) and protease inhibitors). After centrifugation at 10,000 × *g* for 120 min at 4 °C, 1 ml of nickel-nitrilotriacetic acid-agarose beads pre-equilibrated with extraction buffer was added to the supernatant. The mixture was gently agitated overnight at 4 °C. After washing 3 times with 10 ml of washing buffer (50 mM Tris, pH 8.0, 100 mM NaCl, 5 mM imidazole, and 0.2 mM PMSF), Gβγ was eluted with 10 ml of elution buffer (50 mM Tris, pH 8.0, 100 mM NaCl, 10 mM EDTA, and 200 mM imidazole).

Gβγ Binding Assay (with Purified $G\beta_1\gamma_2$ Proteins)—Ten μg of $G\alpha_s$ protein (with an N-terminal GST tag, attached to glutathione beads) were incubated in 100 μl of binding buffer (20 mM Hepes, pH 8.0, 2 mM GDP, 1 mM DTT, 150 mM NaCl, and 0.02% DM) with 100 nM $G\beta_1\gamma_2$ proteins overnight at 4 °C. After centrifugation, beads were washed three times with binding buffer and then eluted with binding buffer containing 10 mM reduced glutathione. After SDS-PAGE, Western blots were performed with anti-$G\alpha_s$ and anti-G_β antibodies (Santa Cruz Biotechnology, Inc.).

Gβγ Binding Assay (with Membrane Preparations)—Membrane preparations were made from 293T cells. After solubilization, the supernatant (in 20 mM Hepes, pH 8.0, 2 mM GDP, 1 mM DTT, 150 mM NaCl, 1% DM, and protease inhibitors) was pre-cleared with glutathione beads. 500 μl of supernatant was mixed with 10 μg of $G\alpha_s$ protein (with an N-terminal GST tag, attached to glutathione beads). The mixtures were rolled at 4 °C overnight. After centrifugation, beads were washed three times with binding buffer and then eluted with binding buffer containing 10 mM reduced glutathione. After SDS-PAGE, Western blots were performed with anti-$G\alpha_s$ and anti-G_β antibodies.

Size Exclusion Chromatography—Size exclusion chromatography was used to examine the binding of $G\alpha_s$ and its mutants to $G\beta_1\gamma_2$ in solution. $G\alpha_s$ (1 μM) and $G\beta_1$(C68S)γ_2 (2 μM) were mixed and incubated on ice for 30 min. Samples were loaded on a Superdex 200 column (GE Healthcare Life Sciences) equilibrated with 20 mM Hepes, pH 8.0, 50 mM NaCl, and 1 mM EDTA at a flow rate of 0.5 ml/min. The elution was monitored at 280 nm, and 0.8-ml fractions were collected for subsequent SDS-PAGE analysis.

In Vivo cAMP Assay—Cells were plated on 6-well plates and treated with 1 mM isobutylmethylxanthine for 30 min at 37 °C. After washing twice with HEM buffer (20 mM Hepes, pH 7.4, 135 mM NaCl, 4.7 mM KCl, 1.2 mM $MgSO_4$, 2.5 mM $NaHCO_3$, 0.1 mM Ro-20–1724, 0.5 unit/ml of adenosine deaminase, and 1 mM isobutylmethylxanthine), cells were treated with 0, 1 nM, 10 nM, 100 nM, 1 μM, 10 μM, and 100 μM isoproterenol in HEM buffer for 5 min at 37 °C. After two additional washes with HEM buffer, cells were harvested and lysed with 0.5% Triton X-100 containing 1 mM isobutylmethylxanthine. The amount of cAMP was measured with a Direct Cyclic AMP Enzyme Immunoassay kit (Assay Designs, Inc.).

In Vitro Adenylyl Cyclase Activation Assay—Adenylyl cyclase activation assay of Sf9 membrane preparations was performed as previously described (22). Briefly, adenylyl cyclase isoform V (dog) was recombinantly expressed in Sf9 cells, and the adenylyl cyclase-containing membranes were prepared. $G\alpha_s$ protein was activated by adding a buffer consisting of 10 mM NaF, 10 mM $MgCl_2$, 30 μM $AlCl_3$ and incubated at 30 °C for 1 h. Activated $G\alpha_s$ proteins with membrane preparations of adenylyl cyclase

V were incubated in buffer of 50 mM Tris, pH 7.6, 2 mM isobutylmethylxanthine, 1 mM ATP, 10 mM $MgCl_2$, 20 mM creative phosphate, 100 units/ml of creative phosphokinase at 30 °C for 10 min. The samples were boiled for 3 min to stop the reaction. After spinning for 3 min at 16,000 × *g*, the supernatant was used for cAMP measurement with Direct Cyclic AMP Enzyme Immunoassay kit.

Purification of Turkey β_1-Adrenergic Receptor Proteins—Turkey β_1-adrenergic receptor protein was purified as described previously (23). Turkey β_1-adrenergic receptor (residues 34–424 with a mutation C116L) cDNA was subcloned into the pVL1393 vector. Hi5 cells were infected with the recombinant baculovirus carrying the turkey β_1-adrenergic receptor at a density of 2×10^6/ml. Sixty-hours later, cells were harvested and resuspended in lysis buffer (50 mM Tris-HCl, pH 8, 1 mM EDTA, 10 μg/ml of leupeptin, 9 mM benzamidine, 5 μg/ml of pepstatin A, and 2 mM PMSF). After homogenization, the cell lysate was centrifuged at 2,000 × *g* for 10 min and the supernatant was centrifuged again at 150,000 × *g* at 4 °C for 1.5 h. The membrane pellet was resuspended in lysis buffer and homogenized again. After spinning down at 150,000 × *g* at 4 °C for 1.5 h, the final pellet was then resuspended in membrane extraction buffer (50 mM Tris-HCl, pH 8, 350 mM NaCl, 3 mM imidazole, 2% DM, 10 μg/ml of leupeptin, 9 mM benzamidine, 5 μg/ml of pepstatin A, and 1 mM PMSF) and rolled at 4 °C for 3 h. After centrifugation at 150,000 × *g* at 4 °C for 1 h, solubilized membrane proteins were incubated with nickel-nitrilotriacetic acid-agarose (Qiagen) overnight. After washing with buffer containing 50 mM Tris-HCl, pH 8, 350 mM NaCl, 3 mM imidazole, 0.1% DM, 10 μg/ml of leupeptin, 9 mM benzamidine, 5 μg/ml of pepstatin A, and 1 mM PMSF, the receptor protein was eluted down by an imidazole gradient.

GTPγS Loading Assay—Agonist-stimulated GTPγS loading to G-proteins was performed as previously described (19). $G\alpha_s$ (with or without 1 μM $G\beta\gamma$) and turkey β_1-adrenergic receptor (20 nM) together with 10 μM alprenolol or isoproterenol in 200 μl of loading buffer (50 mM Tris, pH 8.0, 100 mM NaCl, 10 mM $MgCl_2$, 1 mM EDTA, 0.02% DM, and 5 μM GDP) were incubated on ice for 20 min. After incubation at 30 °C (for wild-type and $G\alpha_s$219) or at room temperature (for $G\alpha_s$263 and $G\alpha_s$195) for 5 min, 100 nM GTPγS was added. At various times, 40-μl aliquots were removed and added to 1 ml of termination buffer (20 mM Tris, pH 8.0, 100 mM NaCl, and 25 mM $MgCl_2$, ice cold) and loaded onto nitrocellulose membrane (Schleicher & Schuell BioScience). After 3 washes with 1 ml of termination buffer, 4 ml of scintillation liquid were added to the membrane and ^{35}S was counted to measure GTPγS loading. 5 mM GDP was used to determine nonspecific binding.

$G\alpha_s$ and Receptor Binding Assay—Different concentrations of $G\alpha_s$ proteins (with an N-terminal GST tag, attached to glutathione beads) were incubated in 100 μl of binding buffer with 80 nM β-AR proteins (with a FLAG tag) at 4 °C for 1 h. GST (600 nM) was used as control. After centrifugation, beads were washed three times with washing buffer. After SDS-PAGE, Western blots were performed with anti-$G\alpha_s$ and anti-FLAG M2 antibodies.

RESULTS AND DISCUSSION

Identification of $G\alpha_s$ Mutants Defective in $G\beta\gamma$ Binding—To identify $G\alpha$ subunits that could be activated by GPCRs in the absence of $G\beta\gamma$ subunits, we first characterized $G\alpha_s$ mutants that were defective in $G\beta\gamma$ binding. The crystal structures of $G\alpha$ and $G\alpha\beta\gamma$ have been solved (24, 25). The conformational differences between the free and $G\beta\gamma$-bound forms of $G\alpha$-GDP mainly involve residues that directly interact with $G\beta$ (24, 25). Based on the crystal structures of $G\alpha_t G\beta_1\gamma_1$ and $G\alpha_{i1} G\beta_1\gamma_2$ complexes, residues in the N-terminal, Switch I (Arg-185 to Ile-193, encompassing Linker 2 region), and Switch II region of $G\alpha$ subunits are involved in contacting or binding of $G\beta\gamma$ (24, 25) (Fig. 1*C*, *red* residues). Furthermore, from the crystal structures of the Ras superfamily GTPases and their guanine nucleotide-exchange factors, such as Ras and Sos1, Arf1 and Sec7, Rac1 and Tiam1, EF-Tu and EF-Ts, as well as Ran and RCC1 (26–30), guanine nucleotide-exchange factors interact extensively with and remodel the Switch I and II regions of GTPases. Therefore, we have performed alanine scanning mutagenesis of every residue in these regions as well as some residues in Switch III and its adjacent regions (Table 1 and Fig. 1*D*).

First we identified $G\alpha_s$ mutants that could not bind $G\beta\gamma$. We purified recombinant proteins of wild-type $G\alpha_s$ and 66 mutant $G\alpha_s$ proteins from *E. coli* (Table 1 and some examples shown in Fig. 2*A*). (Here we used the short spliced variant of bovine $G\alpha_s$. The difference between the short and long splice forms of $G\alpha_s$ is an insertion of 14 amino acids after residue Gly-70.) We also purified recombinant $G\beta_1\gamma_2$ proteins from insect Hi5 cells (Fig. 2*A*). To test the functionality of these purified $G\alpha_s$ mutant proteins, we performed *in vitro* GTPγS binding assays and adenylyl cyclase activation assays for all $G\alpha_s$ mutants (Table 1). Other than eight mutants (Table 1), all $G\alpha_s$ mutant proteins were able to bind to GTPγS, implying these purified proteins were stable and functional. Furthermore, using membrane preparations from Sf9 insect cells infected with recombinant baculoviruses carrying adenylyl cyclase type V, we performed *in vitro* adenylyl cyclase activation assays (Table 1, and some examples shown in Fig. 2, *B–E*). In addition to the 8 mutants that could not bind GTPγS *in vitro*, 4 more mutants could not activate adenylyl cyclase *in vitro* (Table 1). Three (Asn-265, Arg-266, and Trp-267) of these 4 residues are in the α3/β5 loop, which directly contacts the catalytic domain of adenylyl cyclase as revealed by the crystal structure of the complex of $G\alpha_s$ and the catalytic domains of adenylyl cyclase (31). Thus, most of the purified mutant $G\alpha_s$ proteins were stable and functional.

We next tested the interaction of these $G\alpha_s$ mutants with $G\beta\gamma$. For the *in vitro* binding experiments, we incubated wild-type $G\alpha_s$ and mutant $G\alpha_s$ proteins with purified $G\beta_1\gamma_2$ proteins. Glutathione beads were used to pulldown $G\alpha_s$ proteins. Co-precipitation of $G\beta_1\gamma_2$ was detected with anti-$G\beta$ antibody. As shown in Table 1 (and some examples in Fig. 2*F*), wild-type $G\alpha_s$ and 48 mutant $G\alpha_s$ proteins pulled down $G\beta_1\gamma_2$, 18 other mutant $G\alpha_s$ proteins (including $G\alpha_s$E195A, $G\alpha_s$K219A, or $G\alpha_s$W263A) did not bind $G\beta_1\gamma_2$. To confirm these binding data and to show that the 18 mutant $G\alpha_s$ proteins could not interact with other $G\beta$ subunits in addition to $G\beta_1$, we used membrane preparations of 293T cells as the source of $G\beta\gamma$ subunits (293T

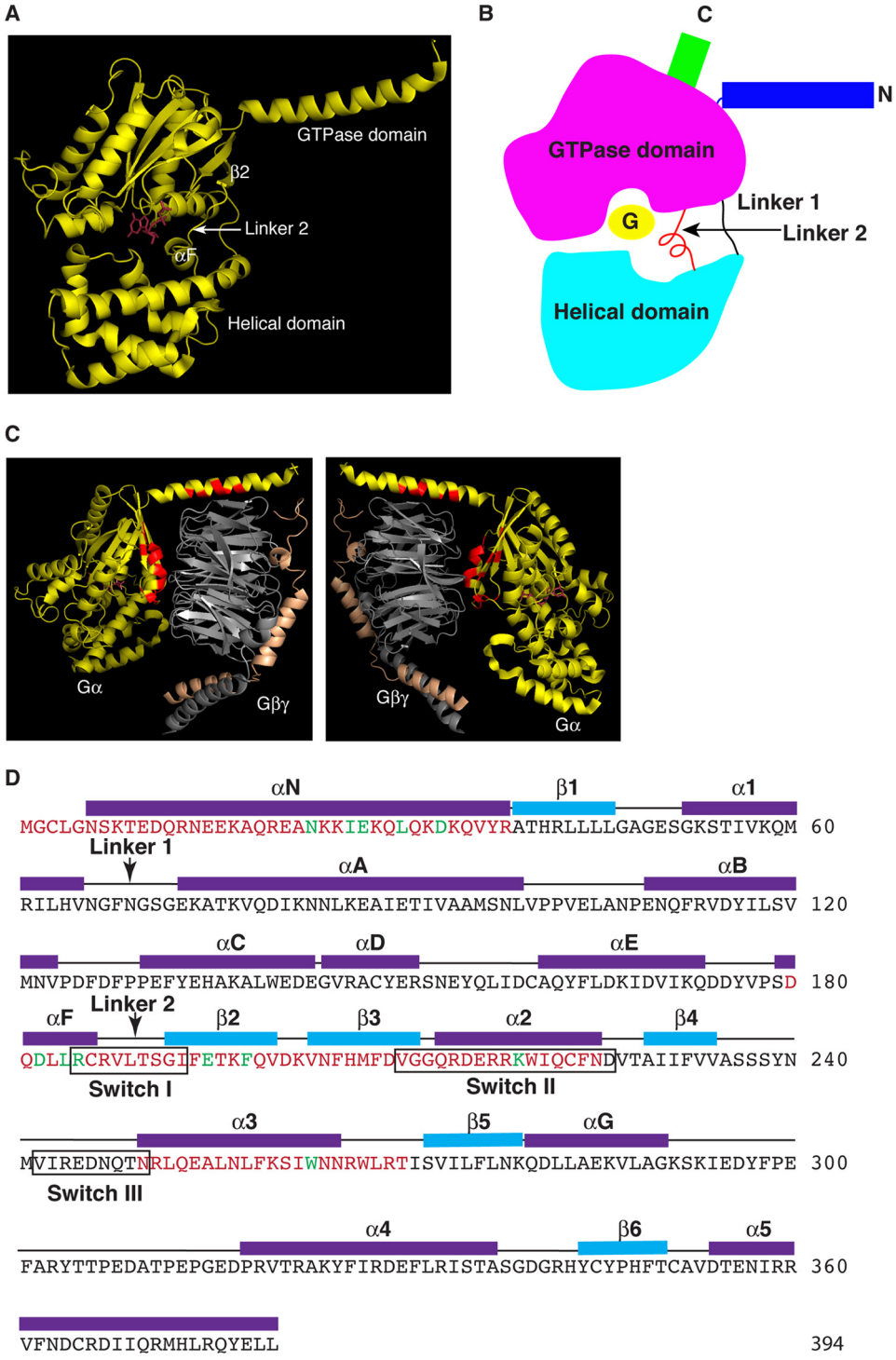

FIGURE 1. **Summary of mutated amino acid residues of $G\alpha_s$.** *A*, crystal structure of a Gα subunit shows the Ras-like GTPase domain and the α-helical domain. The αF, Linker 2, and β2 are indicated. The bound GDP is colored in *magenta*. *B*, diagram of a Gα subunit shows the relative locations of elements discussed in the paper. *C*, all residues on Gα contacting Gβγ are labeled (in *red*) based on crystal structures. The two images are the same rotated 180°. *D*, summary of mutated residues of $G\alpha_s$ (*magenta* and *green letters*). The secondary structure is assigned based on the crystal structure of $G\alpha_s$-GTPγS (PDB code 1AZT). The three switch regions are indicated by *black boxes*. The two linker regions are indicated by *arrows*. *Green* amino acid letters indicate the residues mutated in the 8 $G\alpha_s$ mutants that are activated by β-ARs without Gβγ binding.

cells at least express $G\beta_1$, $G\beta_2$, and $G\beta_4$). The results were the same as the binding experiments with purified $G\beta_1\gamma_2$ (Table 1 and some examples shown in Fig. 2*G*). As a third approach, we used size exclusion chromatography to verify the inability of some $G\alpha_s$ mutants binding to Gβγ. As shown in Fig. 2*H*, wild-type $G\alpha_s$, $G\alpha_s$K219A, and $G\beta_1\gamma_2$ eluted as single major peaks from the size exclusion column, demonstrating the homogeneity of the subunit preparations. When combined with excess $G\beta_1\gamma_2$, wild-type $G\alpha_s$ showed a two-peaks elution profile: one was the free $G\beta_1\gamma_2$ and the other was the complex of $G\alpha_s$-$G\beta_1\gamma_2$ with a shorter retention time as compared with the isolated wild-type $G\alpha_s$ (Fig. 2*H*). On the other hand, $G\alpha_s$K219A

TABLE 1

Summary of the characterization of 66 $G\alpha_s$ mutants

GTPγS binding and *in vitro* activation of adenylyl cyclase (AC) were shown as percentage of the values obtained with wild-type $G\alpha_s$. The increase of cAMP in cells is shown as the fold increase from each individual experiment. ΔN31 and ΔN38 are deletion mutants of the N-terminal 31 or 38 amino acids, respectively.

MUTANTS	GTPγS binding (%)	AC in vitro (%)	AC activation in cells (fold cAMP increase)	Gβγ binding	
				in vitro	in vivo
$G\alpha_s$	100	100	14X, 14X, 8X, 7X, 20X, 20X	YES	YES
D180A	55	50	12X, 15X, 10X, 14X	YES	YES
Q181A	90	40	20X, 30X, 18X, 14X	YES	YES
D182A	NO	NO	4X, 4X, 3X, 3X	NO	NO
L183A	115	35	13X, 9X, 23X, 14X	YES	YES
L184A	NO	NO	2X, 5X, 4X, 4X, 2X, 3X	NO	NO
R185A	10	105	9X, 16X, 8X, 20X	NO	NO
C186A	105	276	12X, 30X, 25X, 20X	YES	YES
R187A	43	22	NO	YES	YES
V188A	100	NO	NO	YES	YES
L189A	100	207	30X, 5X, 10X, 2X	YES	YES
T190A	45	38	9X, 2X, 9X, 2X	YES	YES
L189A/T190A	75	298	NO	YES	YES
S191A	40	118	NO	YES	YES
G192A	25	93	3X, 4X, 8X, 6X	YES	YES
I193A	40	52	NO	YES	YES
F194A	95	76	14x, 12X, 28X, 17x	YES	YES
E195A	35	52	3X, 4X, 7X, 6X	NO	NO
T196A	70	149	NO	YES	YES
K197A	75	48	7X, 5X, 15X, 4X	YES	YES
F198A	NO	NO	4x, 2X, 4X, 3X	NO	NO
Q199A	170	52	10X, 10X, 16X, 14X	YES	YES
V200A	85	71	12X, 24X, 12X, 7x	YES	YES
D201A	55	60	10X, 12X, 9X, 9X	YES	YES
K202A	130	72	22X, 30X, 21X, 44X	YES	YES
V203A	125	91	4X, 6X, 4X, 6X	YES	YES
N204A	55	77	11X, 14X, 14X, 8X	YES	YES
F205A	NO	NO	NO	NO	NO
H206A	90	120	5X, 8X, 8X, 9X	YES	YES
M207A	10	30	18X, 40X, 20X, 20X	YES	YES
F208A	10	20	8X, 11X, 5X, 8X	YES	YES
D209A	50	68	NO	YES	YES
V210A	140	57	6X, 15X, 4X, 7X	YES	YES
G211A	85	38	10X, 24X, 9X, 14X	YES	YES
G212A	55	35	NO	YES	YES
Q213A	40	140	3X, 4X, 3X	YES	YES
R214A	15	107	NO	YES	YES
D215A	50	27	NO	YES	YES
E216A	110	156	20X, 20X, 20X	YES	YES
R217A	70	190	NO	YES	YES
R218A	100	67	NO	YES	YES
K219A	115	78	4X, 5X, 6X, 4X	NO	NO
W220A	100	216	NO	YES	YES
W220R	65	14	NO	NO	NO
I221A	150	261	NO	YES	YES
W220A/I221A	NO	NO	NO	NO	NO
Q222A	45	216	NO	YES	YES
C223A	65	261	8X, 6X, 21X, 10X	YES	YES
F224A	80	45	NO	NO	NO
N225A	85	72	35X, 50X, 15X, 20X, 25X	YES	YES
N257A	30	13	NO	YES	YES
L258A	50	68	9X, 8X, 5X, 6X, 6X	YES	YES
F259A	NO	NO	NO	NO	NO
K260A	105	69	8X, 6X, 10X, 11X	YES	YES
S261A	120	233	NO	YES	YES
I262A	30	428	13X, 7X, 5X, 3X	YES	YES
W263A	40	35	13X, 13X, 21X, 24X	NO	NO
N264A	NO	NO	NO	NO	NO
N265A	95	NO	NO	NO	NO
R266A	20	NO	NO	YES	YES
W267A	45	NO	NO	YES	YES
L268A	110	117	3X, 3X, 8X, 8X	YES	YES
T270A	105	97	20X, 17X, 21X, 7X	YES	YES
W263A/L268 A/R269A	NO	NO	NO	NO	NO
ΔN31	20	146	NO	NO	NO
ΔN38	10	78	NO	NO	NO
N23A/I26A/ E27A/L30A/ D33A	10	75	3X, 3X, 3X, 3X, 3X	NO	NO

showed a two-peak elution prolife with the same retention times as free $G\beta_1\gamma_2$ and free $G\alpha_s$K219A, indicating that $G\beta_1\gamma_2$ had little effect on the retention time of $G\alpha_s$K219A and that $G\alpha_s$K219A was unable to form a complex with $G\beta_1\gamma_2$ (Fig. 2*H*). Similar results were observed with $G\alpha_s$E195A and $G\alpha_s$W263A, which could not form trimers with $G\beta_1\gamma_2$. Together, these data demonstrate that 18 $G\alpha_s$ mutants (including $G\alpha_s$E195A, $G\alpha_s$K219A, and $G\alpha_s$W263A) are unable to interact with $G\beta\gamma$ subunits, and the locations of these 18 $G\alpha_s$ mutants are displaced in Fig. 3 (*red* and *green* residues).

Activation of $G\alpha_s$ Mutants by β-Adrenergic Receptors in Cells—Because our goal was to find $G\alpha_s$ mutants that could be potentially activated by GPCRs in the absence of $G\beta\gamma$, we next investigated the activation of all 66 $G\alpha_s$ mutants by GPCRs in $G\alpha_s$-deficient cells. $G\alpha_s$-deficient mouse embryonic fibroblast (MEF) cells were derived from $G\alpha_s$ knock-out mouse embryos (32, 33). Because exon 2 of the $G\alpha_s$ gene was deleted, none of the two alternative spliced variants of $G\alpha_s$ were present in these $G\alpha_s^{-/-}$ MEF cells (32, 33). We have made stable cell lines with these $G\alpha_s^{-/-}$ MEF cells expressing $G\alpha_s$ and all 66 $G\alpha_s$ mutants (in pcDNA3.1/hygromycin vector). Stimulation of these cells with isoproterenol, which activates the endogenous G_s-coupled β-adrenergic receptors, increased cellular cAMP accumulation in cells expressing wild-type and 37 mutant $G\alpha_s$ proteins (Table 1, and some examples shown in Fig. 4). Among the 18 $G\alpha_s$ mutants that could not interact with $G\beta\gamma$, 8 mutants ($G\alpha_s$D182A, $G\alpha_s$L184A, $G\alpha_s$R185A, $G\alpha_s$E195A, $G\alpha_s$F198A, $G\alpha_s$K219A, $G\alpha_s$W263A, and $G\alpha_s$N23A/I26A/E27A/L30A/D33A) could still mediate receptor activation of adenylyl cyclases leading to cAMP increase (Fig. 4, *B-E*, and *green* in Fig. 1*D*). As control, $G\alpha_s^{-/-}$ MEF cells did not show any cAMP increase upon isoproterenol stimulation (Fig. 4*A*). The functionality of these $G\alpha_s$ mutant proteins was also verified by cholera toxin, a direct activator of $G\alpha_s$ (Fig. 4). These cellular studies demonstrate that 8 $G\alpha_s$ mutants are able to functionally couple to β-adrenergic receptors, are activated by the receptors, and stimulate the downstream effector adenylyl cyclases, leading to the cellular accumulation of cAMP, even though they could not bind to $G\beta\gamma$.

Activation of Purified $G\alpha_s$ Mutants by Purified β-Adrenergic Receptors in Vitro in the Absence of $G\beta\gamma$—To directly demonstrate that a GPCR has the capability to accelerate the guanine-nucleotide exchange on $G\alpha$ without $G\beta\gamma$, we performed biochemical studies with purified recombinant proteins of a GPCR and $G\alpha_s$ mutants *in vitro*. We purified recombinant turkey β_1-adrenergic receptors from insect Hi5 cells (23) (Fig. 5*A*). $G\alpha_s$ proteins were initially purified as GST fusion proteins and the GST tag was removed by protease cleavage (Fig. 5*B*). Among the 8 $G\alpha_s$ mutants identified above (able to be activated by β-AR in cells but unable to bind $G\beta\gamma$), 5 (D182A, L184A, R185A, F198A, and N23A/I26A/E27A/L30A/D33A) were unstable after removal of the GST tag. Therefore, we examined the activation of the remaining 3 $G\alpha_s$ mutants (E195A, K219A, and W263A) by β-adrenergic receptor. The activation was monitored by the initial rate of GTPγS loading onto $G\alpha_s$ subunits. As reported previously, purified β-adrenergic receptors had no effect on the rate of GTPγS loading (~90 fmol/min) onto wild-type $G\alpha_s$ proteins in the absence of $G\beta\gamma$ subunits (19, 34) (Fig. 5*C*). The rate of GTPγS loading on $G\alpha_s$ was the same in the presence of isoproterenol (an agonist for β-adrenergic receptor) or alprenolol (an antagonist). The initial rate of GTPγS loading to $G\alpha_s$ alone was similar to that of $G\alpha_s$ with β-adrenergic receptor in the presence of the antagonist alprenolol. In contrast, in the presence of purified $G\beta\gamma$ proteins, isoproterenol increased the initial rate of GTPγS loading onto $G\alpha_s$ (~450 fmol/min) by 4-fold compared with that in the presence of alprenolol (~115 fmol/min) (Fig. 5*D*). The fold-increase is similar to that reported in previous reconstituted systems, reflecting a relatively high basal nucleotide exchange rate of $G\alpha_s$ (19, 34).

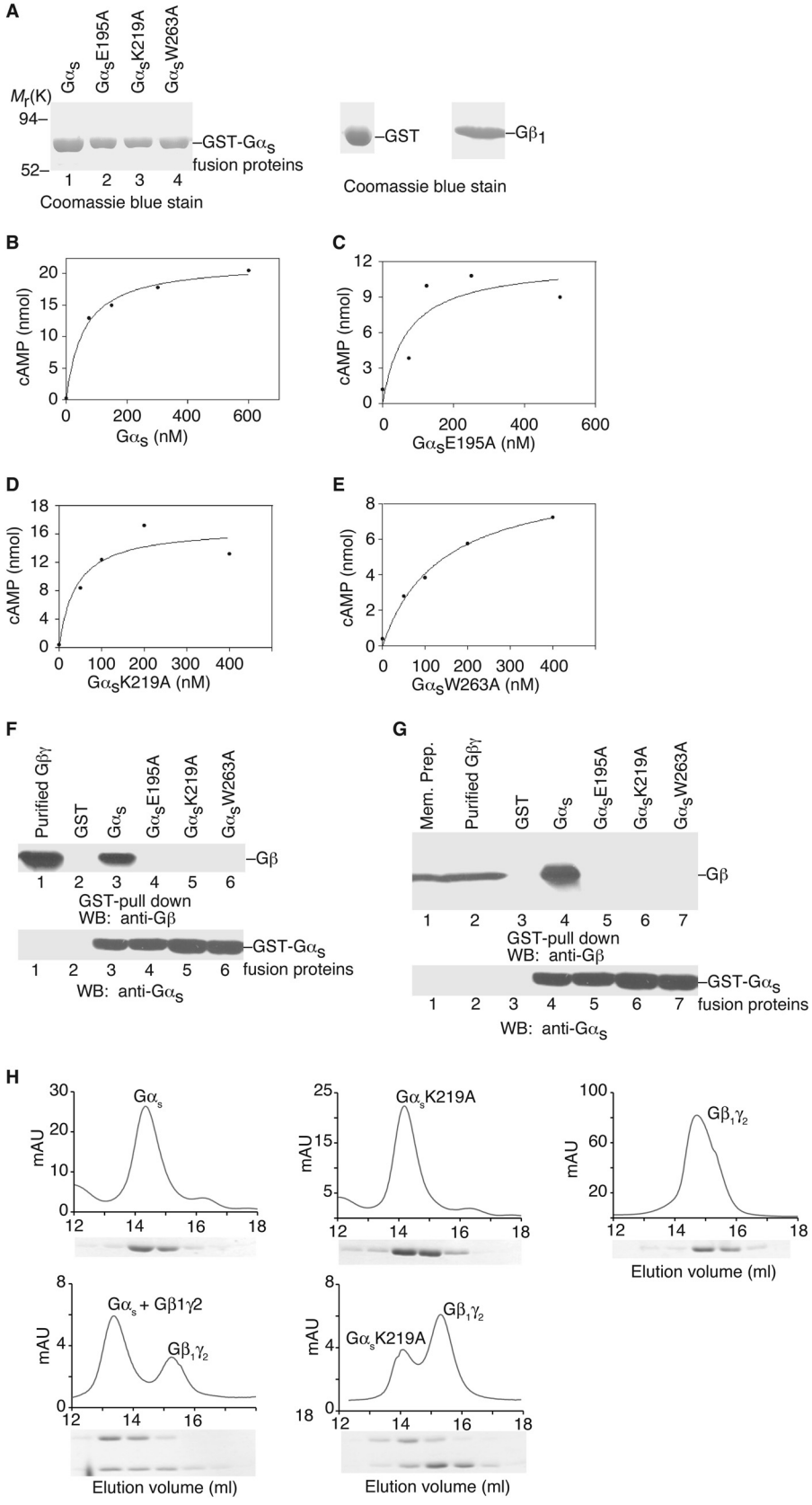

FIGURE 2. **Functional characterization of $G\alpha_s$ and its mutants.** *A*, Coomassie Blue staining shows the purified $G\alpha_s$ proteins (some representatives), GST and $G\beta_1\gamma_2$. *B–E*, *in vitro* activation assays of adenylyyl cyclase by $G\alpha_s$ and its mutants (some representatives). *F* and *G*, *in vitro* binding of $G\alpha_s$ and representative mutants to $G\beta_1\gamma_2$. *H*, size exclusion chromatography of heterotrimer formation. *Upper panels*: elution profiles are shown for wild-type $G\alpha_s$ alone, $G\alpha_s$K219A alone, $G\beta_1\gamma_2$ alone, the mixture of wild-type $G\alpha_s/G\beta_1\gamma_2$, and the mixture of $G\alpha_s$K219A/$G\beta_1\gamma_2$. *Lower panels*, SDS-PAGE analysis of the elution fractions. One representative experiment from three independent experiments is shown for each case. *WB*, Western blot.

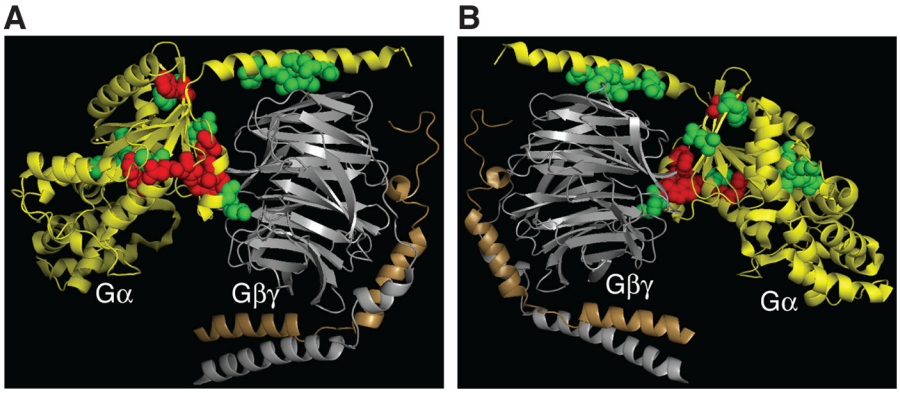

FIGURE 3. **Spatial locations of 18 $G\alpha_s$ mutants that are defective in $G\beta\gamma$ binding.** The structure displayed is $G\alpha_{i1}\beta_1\gamma_2$ (PDB code 1GP2). $G\alpha$, *yellow*; $G\beta$, *gray*; $G\gamma$, *gold*. Corresponding residues for the 18 $G\alpha_s$ mutants are highlighted (*red* and *green*). *Green* labeled residues are the 8 $G\alpha_s$ mutants that are defective in $G\beta\gamma$ binding but can still be activated by β-ARs. *Red* labeled residues are the 10 $G\alpha_s$ mutants that are defective in $G\beta\gamma$ binding and could not be activated by β-ARs. *A* and *B* are the same image rotated 180°.

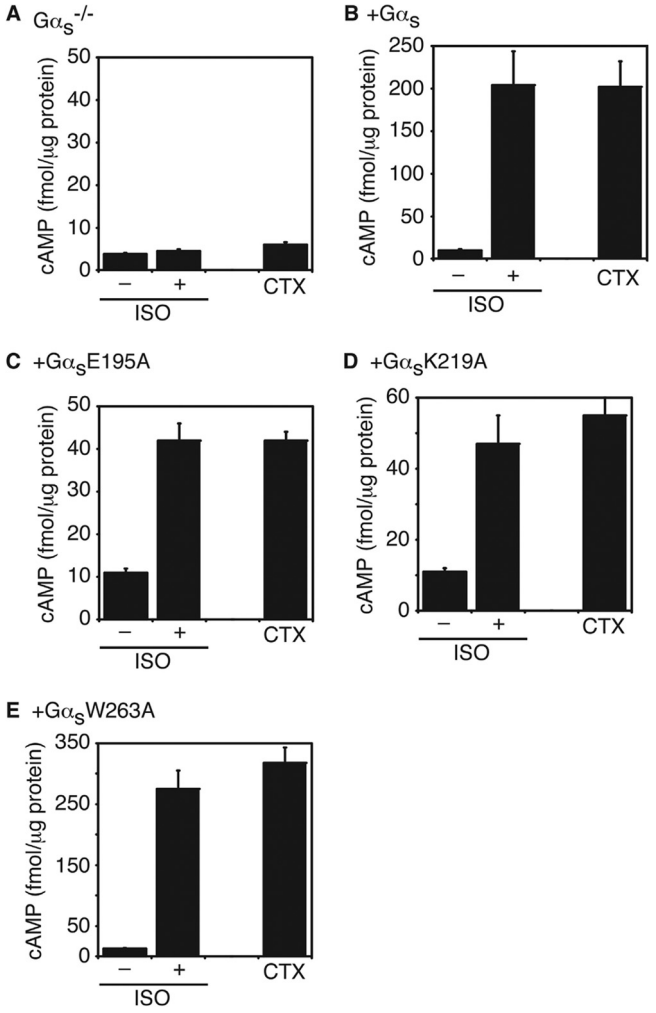

FIGURE 4. ***In vivo* activation of adenylyl cyclase by $G\alpha_s$ and representative mutants.** *A*, isoproterenol (*ISO*) or cholera toxin (*CTX*) failed to increase the cellular cAMP levels in $G\alpha_s^{-/-}$ MEF cells. *B–E*, Both ISO and CTX increased the cellular cAMP levels in $G\alpha_s^{-/-}$ cells stably re-expressing wild-type $G\alpha_s$ (*B*), $G\alpha_s$E195A (*C*), $G\alpha_s$K219A (*D*), or $G\alpha_s$W263A (*E*). Data shown are mean ± S.D. of three independent experiments.

With purified $G\alpha_s$E195A, we found that, without $G\beta\gamma$ subunits, isoproterenol increased the rate of GTPγS loading by about 2.4-fold compared to that with alprenolol (from ~39 fmol/min with alprenolol to ~95 fmol/min with isoproterenol) (Fig. 5*E*). Addition of $G\beta\gamma$ subunits did not significantly change the rates with either isoproterenol (~105 fmol/min) or alprenolol (~40 fmol/min) (Fig. 5*F*). Similar results were obtained with $G\alpha_s$K219A and $G\alpha_s$W263A mutants: without $G\beta\gamma$ subunits, isoproterenol increased the rate of GTPγS loading by 2~3-fold on $G\alpha_s$K219A and $G\alpha_s$W263A mutants, compared to that with alprenolol. Furthermore, the mutations did not seem to alter the interaction between $G\alpha_s$ and β-AR (Fig. 5*G*). Moreover, increasing the concentrations of $G\beta\gamma$ enhanced the initial rate of GTPγS loading onto wild-type $G\alpha_s$, but not $G\alpha_s$K219A (Fig. 5*H*). Additionally, increasing the concentrations of β-AR elevated the initial rate of GTPγS loading onto both wild-type $G\alpha_s$ (in the presence of $G\beta_1\gamma_2$) and $G\alpha_s$K219A (in the absence of $G\beta_1\gamma_2$) (Fig. 5*H*). These biochemical experiments clearly demonstrate that purified β_1-adrenergic receptors can accelerate the guanine nucleotide exchange on $G\alpha_s$ in the absence of $G\beta\gamma$ subunits. We should note that previous studies with rhodopsin and transducin had indicated that high concentrations of rhodopsin might activate transducin in the absence of $G\beta\gamma$, and that $G\beta_1$ or $G\gamma_1$ knock-out mice still had some light response (35–40). Thus, GPCRs possess the ability to catalyze the nucleotide exchange on $G\alpha$ subunits.

Role of Extended Linker 2 in $G\alpha$ Activation—How do the 8 $G\alpha_s$ mutations ($G\alpha_s$D182A, $G\alpha_s$L184A, $G\alpha_s$R185A, $G\alpha_s$E195A, $G\alpha_s$F198A, $G\alpha_s$K219A, $G\alpha_s$W263A, and $G\alpha_s$N23A/I26A/E27A/L30A/D33A) alleviate the requirement of $G\beta\gamma$ for the activation of $G\alpha_s$ by β-adrenergic receptors? When mapped onto the crystal structure of the complex of β_2-AR and G_s, 3 of these 8 residues (Asp-182, Leu-184, and Arg-185) are in αF helix (Fig. 6 *A* and *B*). Two of the 8 residues (E195 and F198) are in β2 sheet (Fig. 6*B*). αF and β2 flank Linker 2, which connects the Ras-like GTPases domain and the α-helical domain of $G\alpha_s$ (Figs. 6, *A* and *B*, and 1*D*). Also, within Linker 2, mutations of Arg-187, Leu-189/Thr-190, Ile-193, and Thr-196 all blocked β-AR induced cAMP increases in cells even though these mutants could bind to $G\beta\gamma$, GTPγS, and activate adenylyl cyclase *in vitro* (Table 1). Hence, almost all residues in the extended Linker 2 are critical for $G\alpha$ activation. Although some mutations (such as R185A and E195A) enable $G\alpha$ activation by

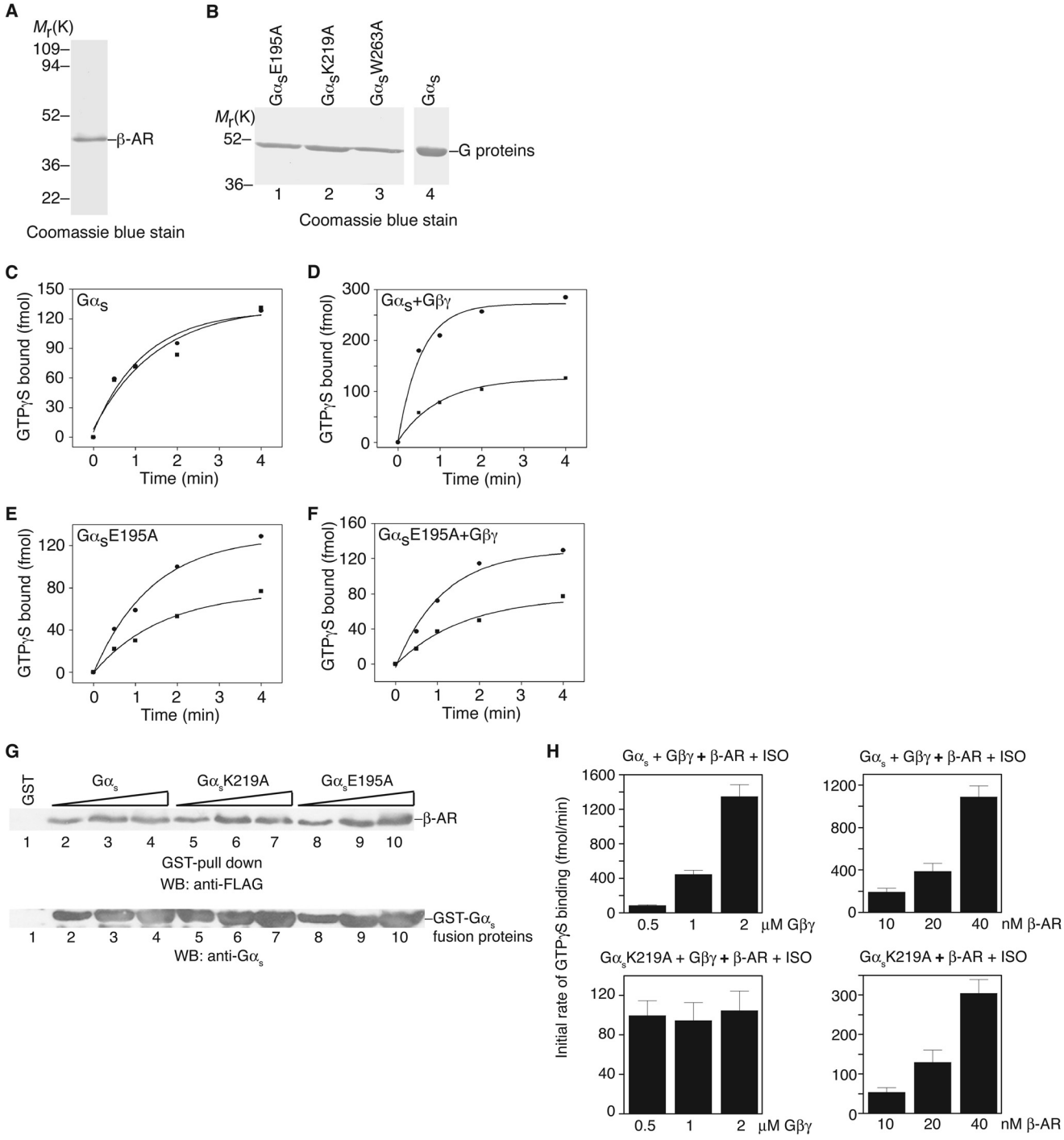

FIGURE 5. ***In vitro* activation of $G\alpha_s$ by the *β*-adrenergic receptor.** *A*, Coomassie Blue staining shows the purified turkey *β*-adrenergic receptor. *B*, Coomassie Blue staining shows some examples of purified G proteins (after GST cleavage). *C*, activation of $G\alpha_s$ by the *β*-adrenergic receptor in the presence of alprenolol (■) or isoproterenol (●). *D*, activation of $G\alpha_s$ + $G\beta_1\gamma_2$ by the *β*-adrenergic receptor in the presence of alprenolol (■) or isoproterenol (●). *E*, activation of $G\alpha_s$E195 by the *β*-adrenergic receptor in the presence of alprenolol (■) or isoproterenol (●). *F*, activation of $G\alpha_s$E195 + $G\beta_1\gamma_2$ by the *β*-adrenergic receptor in the presence of alprenolol (■) or isoproterenol (●). *G*, *in vitro* binding of $G\alpha_s$ and representative mutants to *β*-AR. Different concentrations (150, 300, and 500 nM) of $G\alpha_s$ and mutant proteins were used. *H*, *left two panels*, measurement of the initial rate of GTPγS loading onto wild-type $G\alpha_s$ (*top panel*) or $G\alpha_s$K219A mutant (*bottom panel*) in the presence of different concentrations of $G\beta_1\gamma_2$. *Right two panels*, measurement of the initial rate of GTPγS loading onto wild-type $G\alpha_s$ in the presence of $G\beta_1\gamma_2$ (*top panel*) or the $G\alpha_s$K219A mutant (*bottom panel*) in the absence of $G\beta_1\gamma_2$. One representative experiment from three independent experiments is shown for *A-G*. In *H*, data are shown as mean ± S.E.

GPCR in the absence of Gβγ, other mutations (such as S191A and I193A) block Gα activation by GPCR in cells. When comparing the structures of inactive $G\alpha_i$-GDP and active $G\alpha_i$-GTPγS, or the structures of inactive $G\alpha_t$-GDP and active $G\alpha_t$-GTPγS, Linker 2 is moved toward the γ-phosphate, bringing the side chain oxygen of Thr-190 into the coordination sphere of the Mg^{2+} ion where it replaces one of the water molecules observed in the structure of the GDP form (24, 25). Furthermore, it has been shown that Linker 2 changes the conformation upon GPCR activation (41).

A critical role for the extended Linker 2 in Gα activation is consistent with the observation from the crystal structure of the complex of β_2-AR and G_s, which shows a large rotation (~127°) of the α-helical domain relative to the Ras-like GTPase domain upon G-protein activation (Fig. 6, *A* and *E*) (10). αF/Linker 2, through the β_2-strand, is connected to the β_2/β_3 loop, which interacts with intracellular loop 2 of β_2-AR (Fig. 6*F*). Furthermore, experiments using various biophysical measurements

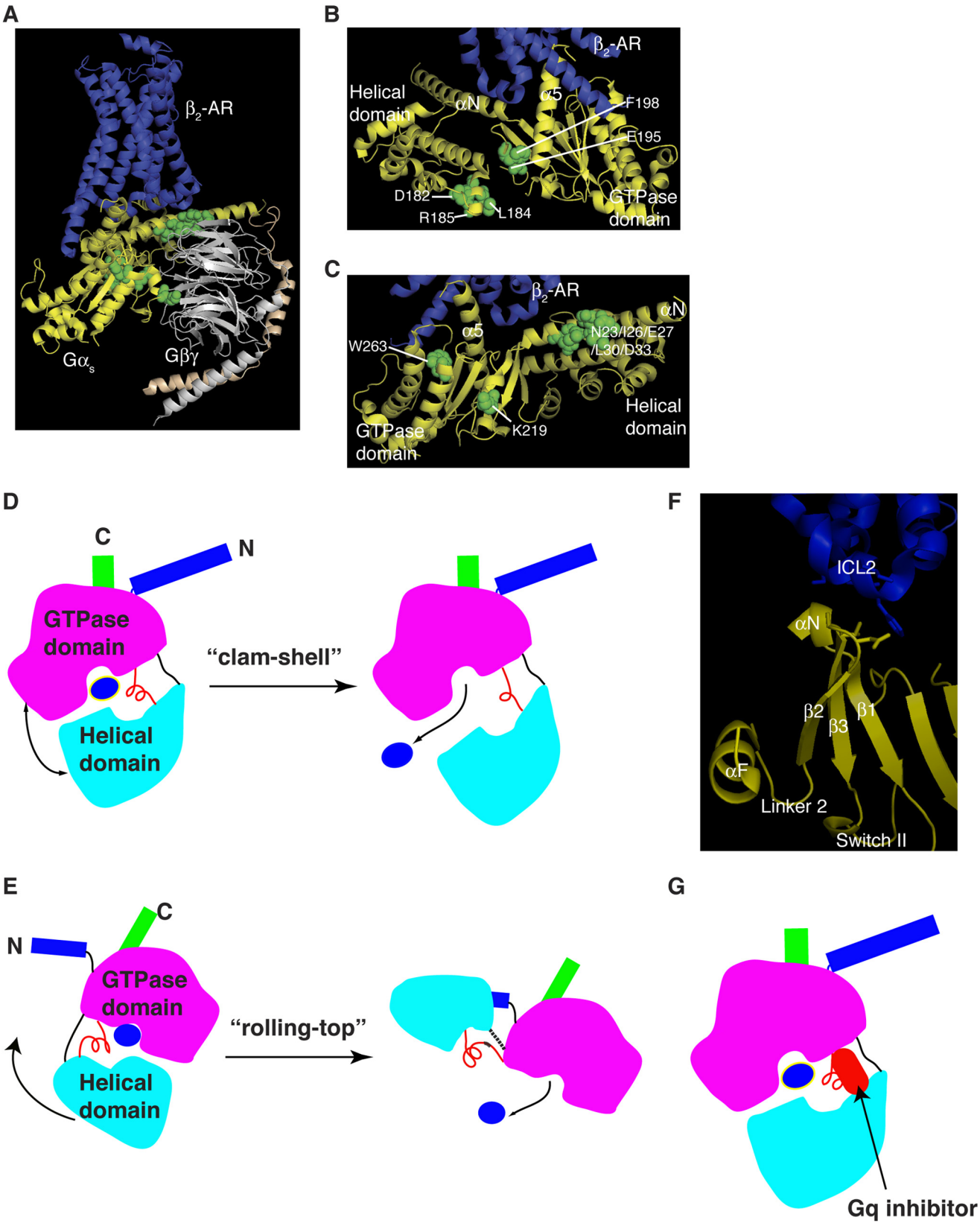

suggest a "clam-shell" like opening model for Gα activation by GPCRs, in which the helical domain opens away from the Ras-like GTPase domain (42–45) (Fig. 6*D*). Here the clustering of several $G\alpha_s$ mutants critical for GPCR activation of $G\alpha_s$ around the extended Linker 2 suggests a possibility that Linker 2 may serve as the "hinge" in this clam-shell model (Fig. 6*D*). Similarly, in the "rolling-top" model (in which the α-helical domain slides and rotates away along the sideways from the Ras-like GTPase domain) observed in the β_2-AR·G_s complex structure, this hinge is stretched (some residues in the linkers were disordered and thus were unmodeled in the structure) (10)(Fig. 6*E*). Mutations of residues in this hinge could make it easy to open the interface between the two domains of Gα or to enhance the interdomain motions. Preventing this interdomain opening by cross-linking inhibits GPCR-catalyzed G-protein activation (42). We should note that, in addition to Linker 2, Linker 1 also connects the Ras-like GTPase domain and the α-helical domain. Indeed a point mutation (G56P) in Linker 1 of transducin increased the basal exchange rate and exhibited some degrees of activation at high levels of rhodopsin in the absence of $\beta_1\gamma_1$ (35). The role of Linker 1 in Gα-protein activation by GPCRs requires future systematic investigation. Here we propose that a GPCR via its intracellular loop 2 directly interacts with the β_2/β_3 loop of Gα to communicate to Linker 2 and αF, resulting in the rotation of the helical domain and the release of GDP (Fig. 6, *E* and *F*).

Linker 2 as the Target Site of a Natural Product Inhibitor for G_q—The crystal structure of G_q and a small molecule natural product inhibitor shows the inhibitor binds to a hydrophobic cleft and directly contacts Linker 2 (Fig. 6*G*) (46). This inhibitor, YM-254890, inhibits the guanine-nucleotide exchange reaction by preventing the GDP release (46). Also, this inhibitor blocks the AlF_4^--induced conformational change in $G\alpha_q$ (46). It is proposed that this inhibitor stabilizes an inactive GDP-bound form (46). These structural data suggest that Linker 2 might be critical for G-protein activation, and that the Linker 2 region is a potential therapeutic targeting site.

Role of αN, α3, and Switch Regions in Gα Activation in Cells—In addition to the extended Linker 2, our data have uncovered some other residues that are essential for $G\alpha_s$ activation in cells by β-ARs. The N-terminal residues (Asn-23, Ile-26, Glu-27, Leu-30, and Asp-33) and Trp-263 are located at or close to the receptor-interacting surface (10, 15, 47, 48)(Fig. 6, *A* and *C*). Trp-263 is close to the α_3/β_5 loop. This region is analogous to GEF contact sites in other GTPases such as Ras and EF-Tu (26, 27). The crystal structure of β_2-AR/G_s has revealed that β_2-AR interacts with the $\alpha N/\beta_1$ hinge; this may explain the role of the 5 N-terminal residues (Asn-23, Ile-26, Glu-27, Leu-30, and Asp-33) in the activation of Gα by GPCR.

Lys-219 is located within Switch II (Figs. 1*D* and 6*C*). Lys-206 of $G\alpha_t$ (corresponding to Lys-219 in $G\alpha_s$) had been identified to be important for $G\alpha_t$ activation by rhodopsin (49). Several residues near Lys-219 of $G\alpha_s$ such as Gly-212 and Gln-213 are critical for triggering conformational changes in Switch II through an interaction with the γ-phosphate in GTP and for stabilizing the transition state for GTP hydrolysis, respectively (13, 14, 50, 51). Indeed, most $G\alpha_s$ mutations in the Switch I and II regions (such as Ile-193, Thr-196, Asp-209, Gly-212, Arg-214, Asp-215, Arg-217, Arg-218, Trp-220, Ile-221, and Gln-222) could not be activated by β-adrenergic receptors in cells, despite their ability to bind to Gβγ subunits, bind to GTPγS, and activate adenylyl cyclases *in vitro* (Table 1). Arg-187 and Thr-190 (in Switch I) as well as Gly-212 (in Switch II) contact the γ-phosphate of GTP (6). Together, these data demonstrate that αN, α3, Switch I and Switch II are critical for Gα activation by GPCRs.

The critical role of Switch I and II regions in Gα activation is similar to the activation of Ras-superfamily GTPases by their GEFs. GEFs for small GTPases have different structures (26–30). They contact GTPases at the same as well as different amino acid residues and induce different conformational changes on GTPases to drive out the GDP. However, they all utilize a two-sided attack to release positive charges (the Mg^{2+} ion and the invariant lysine residue in the P loop (phosphate-binding loop)) from their interaction with the phosphates of the nucleotide (52). These GEFs interact extensively with and remodel Switch I and II regions of GTPases, which form part of the binding pocket for Mg^{2+} and the γ-phosphate of GTP. Thus, although GPCRs are unusual GEFs because they do not contact these switch regions directly, they still require/remodel these switch regions for the activation of Gα.

Possible Role of Gβγ in Gα Activation—Our mutagenesis studies unexpectedly reveal a role for residues Trp-263 (in α3) and Asn-265 (in the α3-β5 loop) in Gβγ binding (Table 1). From the structure of the $G\alpha_i$·GDP/Gβγ complex, this region is not directly involved in contacting with Gβγ. However, this region is right next to Switch III and forms an elaborate interdependent network of polar interactions with the Switch II region, which is critical for interacting with Gβγ (24). Although we did not address the role of Gβγ in the guanine-nucleotide exchange on Gα, we should mention that there were two models that proposed a catalytic role for Gβγ (15, 16, 21). Gβγ subunits contact the switch regions of Gα subunits (24, 25), and have a structure similar to RCC1 (30). Hence, Gβγ subunits would be more like GEFs if only Gβγ subunits could be proven to possess GEF activity without GPCRs. The role of Gβγ in Gα activation could be complex. Gβγ stabilizes GDP binding on Gα, thus serving as a guanine-nucleotide dissociation inhibitor.

FIGURE 6. **Diagrams of Gα activation by GPCRs.** *A*, ribbon presentation of 8 $G\alpha_s$ mutants that are defective in Gβγ binding, but are still activated by β-adrenergic receptors in cells. The structure displayed is the complex of β_2-AR·G_s (PDB code 3SN6). β_2-AR, *dark blue*; $G\alpha_s$, *yellow*; Gβ, *gray*; Gγ, *gold*. Residues in the 8 $G\alpha_s$ mutants (that are defective in Gβγ binding, but are still activated by β-adrenergic receptors in cells) are in *green*. *B*, detailed view of the 5 residues in the αF/Linker 2/β2 region. *C*, detailed view of the residues from the other 3 $G\alpha_s$ mutants. These figures were drawn with MolScript and Raster three-dimensional programs. *D*, diagram of the clam-shell model of Gα activation. The helical domain opens away from the Ras-like GTPase domain, allowing GDP released. *E*, diagram of the rolling-top model of Gα activation. The helical domain (the *top*) slides and rotates away from the Ras-like GTPase domain, leading to GDP release. *Dashed lines* are unmodeled residues in the β_2-AR/G_s structure. *F*, zoomed view of the link from ICL2 of β_2-AR to the αF/Linker 2/β2 region of $G\alpha_s$ from the structure of the β_2-AR·G_s complex. Some parts of $G\alpha_s$ were removed for clarity. *ICL2*, intracellular loop 2 of β_2-AR. *G*, diagram of $G\alpha_q$ with its inhibitor of YM-254890.

GPCR activation could release the inhibition of Gβγ. However, the nucleotide exchange rate of Gα, in the absence of Gβγ, is still slower than that in the presence of GPCRs. This would indicate that, in addition to releasing Gβγ, GPCRs act on the nucleotide exchange on Gα. Gβγ subunits could serve an additional catalytic role to augment the complex formation between GPCRs and Gα subunits, similar to the role of ELMO in facilitating nucleotide exchange on Rac by Dock180 (53). Indeed, our data (Table 1, Fig. 5, *E* and *F*) show that, whereas $G\alpha_s$E195A could be activated by β-ARs in the absence of Gβγ, the extent of activation was suboptimal relative to wild-type $G\alpha_s$ in the presence of Gβγ. This implies that Gβγ somehow contributes to the activation process.

Previously two models were proposed for a catalytic role for Gβγ subunits in activating Gα subunits. In the "lever" model (15, 21), GPCRs cause a tilt (or a rotation) of Gβγ relative to Gα. The membrane proximal part (interacting with the Gα N-terminal helix) of Gβγ moves closer to Gα. The opposite end of Gβγ moves away from Gα and, at the same time, pulls along the interacting parts of Gα. These interacting residues from Switch I and II of Gα are part of the lip of the nucleotide binding pocket. Therefore, GDP can exit permitting exchange by GTP. In the second "gear shift" model (16), GPCRs also cause a tilt of Gβγ. However, the rotating direction is opposite of that in the lever model. Gβγ moves closer to Gα. The N terminus of Gγ (the membrane distal end of Gβγ) moves to contact and displace the helical domain of Gα, creating an exit route for GDP. The exact role of Gβγ in the exchange reaction needs further investigation.

Conclusions—Upon ligand-binding, GPCRs initiate the exchange of GDP bound on Gα subunits of G-proteins with GTP. However, the detailed molecular mechanisms by which GPCRs activate G-proteins are not well understood. Here we reveal some new insights on this process. We demonstrate that a GPCR could activate some Gα mutants in the absence of Gβγ, and that the extended Linker 2 in Gα is critical for Gα activation by GPCRs. These data will advance our understanding of this critical cellular signaling process.

The closed and open states of the cleft (the GDP/GTP binding site) are determined by relative pivoting of the Ras-GTPase domain and the α-helical domain at Linker 2. The closed state of the cleft is represented in all crystal structures of Gα subunits. One of the open states of the cleft is captured in the β_2-AR/G_s crystal structure. This model of activation of Gα subunits suggests that factors binding at the interface of the Ras-GTPase domain and the helical domain might facilitate cleft closure, thus serving as an inhibitor of Gα activation (Fig. 6*G*). Given this pivot model, the two domains of Gα could be either clam-shell opening or rolling-top expansion including a relative rotation of the GTPase domain and the helical domain around an axis through the linkers (Fig. 6, *D* and *E*). Results from several biophysical studies are consistent with the clam-shell opening, and that the crystal structure of the β_2-AR·G_s complex is in line with the rolling-top movement. Therefore, in addition to the established role for α5-helix of Gα connecting GPCRs to the guanine-nucleotide binding pocket, we show here that the extended Linker 2 connects GPCRs to the nucleotide binding pocket as well as the α-helical domain of Gα. In conclusion, our data demonstrate that GPCRs possess the capability to catalyze the nucleotide exchange on Gα subunits, and that the extended Linker 2 is critical for Gα activation by GPCRs.

Acknowledgments—We thank Drs. Lonny Levin and Tom Sakmar and members of our laboratory for helpful comments and discussion.

REFERENCES

1. Rosenbaum, D. M., Rasmussen, S. G., and Kobilka, B. K. (2009) The structure and function of G-protein-coupled receptors. *Nature* **459,** 356–363
2. Pierce, K. L., Premont, R. T., and Lefkowitz, R. J. (2002) Seven-transmembrane receptors. *Nat. Rev. Mol. Cell Biol.* **3,** 639–650
3. Gilman, A. G. (1987) G proteins: transducers of receptor-generated signals. *Annu. Rev. Biochem.* **56,** 615–649
4. Bourne, H. R., Sanders, D. A., and McCormick, F. (1990) The GTPase superfamily: a conserved switch for diverse cell functions. *Nature* **348,** 125–132
5. Simon, M. I., Strathmann, M. P., and Gautam, N. (1991) Diversity of G proteins in signal transduction. *Science* **252,** 802–808
6. Sprang, S. R., Chen, Z., and Du, X. (2007) Structural basis of effector regulation and signal termination in heterotrimeric Gα proteins. *Adv. Protein Chem.* **74,** 1–65
7. Tesmer, J. J. (2010) The quest to understand heterotrimeric G protein signaling. *Nat. Struct. Mol. Biol.* **17,** 650–652
8. Choe, H. W., Park, J. H., Kim, Y. J., and Ernst, O. P. (2011) Transmembrane signaling by GPCRs: insight from rhodopsin and opsin structures. *Neuropharmacology* **60,** 52–57
9. Katritch, V., Cherezov, V., and Stevens, R. C. (2013) Structure-function of the G protein-coupled receptor superfamily. *Annu. Rev. Pharmacol. Toxicol.* **53,** 531–556
10. Rasmussen, S. G., DeVree, B. T., Zou, Y., Kruse, A. C., Chung, K. Y., Kobilka, T. S., Thian, F. S., Chae, P. S., Pardon, E., Calinski, D., Mathiesen, J. M., Shah, S. T., Lyons, J. A., Caffrey, M., Gellman, S. H., Steyaert, J., Skiniotis, G., Weis, W. I., Sunahara, R. K., and Kobilka, B. K. (2011) Crystal structure of the β2 adrenergic receptor-G_s protein complex. *Nature* **477,** 549–555
11. Ramachandran, S., and Cerione, R. A. (2006) How GPCRs hit the switch. *Nat. Struct. Mol. Biol.* **13,** 756–757
12. Schwartz, T. W., and Sakmar, T. P. (2011) Structural biology: snapshot of a signalling complex. *Nature* **477,** 540–541
13. Noel, J. P., Hamm, H. E., and Sigler, P. B. (1993) The 2.2 A crystal structure of transducin-α complexed with GTPγS. *Nature* **366,** 654–663
14. Coleman, D. E., Berghuis, A. M., Lee, E., Linder, M. E., Gilman, A. G., and Sprang, S. R. (1994) Structures of active conformations of $G\alpha_{i1}$ and the mechanism of GTP hydrolysis. *Science* **265,** 1405–1412
15. Iiri, T., Farfel, Z., and Bourne, H. R. (1998) G-protein diseases furnish a model for the turn-on switch. *Nature* **394,** 35–38
16. Cherfils, J., and Chabre, M. (2003) Activation of G-protein Galpha subunits by receptors through Gα-Gβ and Gα-Gγ interactions. *Trends Biochem. Sci* **28,** 13–17
17. Bourne, H. R. (1997) How receptors talk to trimeric G proteins. *Curr. Opin. Cell Biol.* **9,** 134–142
18. Fung, B. K. (1983) Characterization of transducin from bovine retinal rod outer segments: I. separation and reconstitution of the subunits. *J. Biol. Chem.* **258,** 10495–10502
19. Florio, V. A., and Sternweis, P. C. (1989) Mechanisms of muscarinic receptor action on G_o in reconstituted phospholipid vesicles. *J. Biol. Chem.* **264,** 3909–3915
20. Higashijima, T., Ferguson, K. M., Sternweis, P. C., Smigel, M. D., and Gilman, A. G. (1987) Effects of Mg^{2+} and the βγ-subunit complex on the interactions of guanine nucleotides with G proteins. *J. Biol. Chem.* **262,** 762–766
21. Rondard, P., Iiri, T., Srinivasan, S., Meng, E., Fujita, T., and Bourne, H. R. (2001) Mutant G protein α subunit activated by Gβγ: a model for receptor activation? *Proc. Natl. Acad. Sci. U.S.A.* **98,** 6150–6155
22. Steegborn, C., Litvin, T. N., Hess, K. C., Capper, A. B., Taussig, R., Buck, J.,

Levin, L. R., and Wu, H. (2005) A novel mechanism for adenylyl cyclase inhibition from the crystal structure of its complex with catechol estrogen. *J. Biol. Chem.* **280,** 31754–31759
23. Huang, J., Chen, S., Zhang, J. J., and Huang, X. Y. (2013) Crystal structure of oligomeric β1-adrenergic G protein-coupled receptors in ligand-free basal state. *Nat Struct Mol Biol* **20,** 419–425
24. Wall, M. A., Coleman, D. E., Lee, E., Iñiguez-Lluhi, J. A., Posner, B. A., Gilman, A. G., and Sprang, S. R. (1995) The structure of the G protein heterotrimer G_i α1β1γ2. *Cell* **83,** 1047–1058
25. Lambright, D. G., Sondek, J., Bohm, A., Skiba, N. P., Hamm, H. E., and Sigler, P. B. (1996) The 2.0-Å crystal structure of a heterotrimeric G protein. *Nature* **379,** 311–319
26. Kawashima, T., Berthet-Colominas, C., Wulff, M., Cusack, S., and Leberman, R. (1996) The structure of the *Escherichia coli* EF-Tu·EF-Ts complex at 2.5-Å resolution. *Nature* **379,** 511–518
27. Boriack-Sjodin, P. A., Margarit, S. M., Bar-Sagi, D., and Kuriyan, J. (1998) The structural basis of the activation of Ras by Sos. *Nature* **394,** 337–343
28. Goldberg, J. (1998) Structural basis for activation of ARF GTPase: mechanisms of guanine nucleotide exchange and GTP-myristoyl switching. *Cell* **95,** 237–248
29. Worthylake, D. K., Rossman, K. L., and Sondek, J. (2000) Crystal structure of Rac1 in complex with the guanine nucleotide exchange region of Tiam1. *Nature* **408,** 682–688
30. Renault, L., Kuhlmann, J., Henkel, A., and Wittinghofer, A. (2001) Structural basis for guanine nucleotide exchange on Ran by the regulator of chromosome condensation (RCC1). *Cell* **105,** 245–255
31. Tesmer, J. J., Sunahara, R. K., Gilman, A. G., and Sprang, S. R. (1997) Crystal structure of the catalytic domains of adenylyl cyclase in a complex with $G_s\alpha$:GTPγS (see comments). *Science* **278,** 1907–1916
32. Bastepe, M., Gunes, Y., Perez-Villamil, B., Hunzelman, J., Weinstein, L. S., and Jüppner, H. (2002) Receptor-mediated adenylyl cyclase activation through XLα(s), the extra-large variant of the stimulatory G protein α-subunit. *Mol. Endocrinol.* **16,** 1912–1919
33. Sun, Y., Huang, J., Xiang, Y., Bastepe, M., Jüppner, H., Kobilka, B. K., Zhang, J. J., and Huang, X. Y. (2007) Dosage-dependent switch from G protein-coupled to G protein-independent signaling by a GPCR. *EMBO J.* **26,** 53–64
34. Pedersen, S. E., and Ross, E. M. (1982) Functional reconstitution of β-adrenergic receptors and the stimulatory GTP-binding protein of adenylate cyclase. *Proc. Natl. Acad. Sci. U.S.A.* **79,** 7228–7232
35. Singh, G., Ramachandran, S., and Cerione, R. A. (2012) A constitutively active Gα subunit provides insights into the mechanism of G protein activation. *Biochemistry* **51,** 3232–3240
36. Phillips, W. J., Wong, S. C., and Cerione, R. A. (1992) Rhodopsin/transducin interactions: II. influence of the transducin-$\beta\gamma$ subunit complex on the coupling of the transducin-α subunit to rhodopsin. *J. Biol. Chem.* **267,** 17040–17046
37. Herrmann, R., Heck, M., Henklein, P., Hofmann, K. P., and Ernst, O. P. (2006) Signal transfer from GPCRs to G proteins: role of the Gα N-terminal region in rhodopsin-transducin coupling. *J. Biol. Chem.* **281,** 30234–30241
38. Lobanova, E. S., Finkelstein, S., Herrmann, R., Chen, Y. M., Kessler, C., Michaud, N. A., Trieu, L. H., Strissel, K. J., Burns, M. E., and Arshavsky, V. Y. (2008) Transducin γ-subunit sets expression levels of α- and β-subunits and is crucial for rod viability. *J. Neurosci.* **28,** 3510–3520
39. Kolesnikov, A. V., Rikimaru, L., Hennig, A. K., Lukasiewicz, P. D., Fliesler, S. J., Govardovskii, V. I., Kefalov, V. J., and Kisselev, O. G. (2011) G-protein $\beta\gamma$-complex is crucial for efficient signal amplification in vision. *J. Neurosci.* **31,** 8067–8077
40. Nikonov, S. S., Lyubarsky, A., Fina, M. E., Nikonova, E. S., Sengupta, A., Chinniah, C., Ding, X. Q., Smith, R. G., Pugh, E. N., Jr., Vardi, N., and Dhingra, A. (2013) Cones respond to light in the absence of transducin β subunit. *J. Neurosci.* **33,** 5182–5194
41. Oldham, W. M., Van Eps, N., Preininger, A. M., Hubbell, W. L., and Hamm, H. E. (2007) Mapping allosteric connections from the receptor to the nucleotide-binding pocket of heterotrimeric G proteins. *Proc. Natl. Acad. Sci. U.S.A.* **104,** 7927–7932
42. Van Eps, N., Preininger, A. M., Alexander, N., Kaya, A. I., Meier, S., Meiler, J., Hamm, H. E., and Hubbell, W. L. (2011) Interaction of a G protein with an activated receptor opens the interdomain interface in the α subunit. *Proc. Natl. Acad. Sci. U.S.A.* **108,** 9420–9424
43. Chung, K. Y., Rasmussen, S. G., Liu, T., Li, S., DeVree, B. T., Chae, P. S., Calinski, D., Kobilka, B. K., Woods, V. L., Jr., and Sunahara, R. K. (2011) Conformational changes in the G protein G_s induced by the β2 adrenergic receptor. *Nature* **477,** 611–615
44. Westfield, G. H., Rasmussen, S. G., Su, M., Dutta, S., DeVree, B. T., Chung, K. Y., Calinski, D., Velez-Ruiz, G., Oleskie, A. N., Pardon, E., Chae, P. S., Liu, T., Li, S., Woods, V. L., Jr., Steyaert, J., Kobilka, B. K., Sunahara, R. K., and Skiniotis, G. (2011) Structural flexibility of the $G\alpha_s$ α-helical domain in the β_2-adrenoceptor G_s complex. *Proc. Natl. Acad. Sci. U.S.A.* **108,** 16086–16091
45. Jones, J. C., Jones, A. M., Temple, B. R., and Dohlman, H. G. (2012) Differences in intradomain and interdomain motion confer distinct activation properties to structurally similar Gα proteins. *Proc. Natl. Acad. Sci. U.S.A.* **109,** 7275–7279
46. Nishimura, A., Kitano, K., Takasaki, J., Taniguchi, M., Mizuno, N., Tago, K., Hakoshima, T., and Itoh, H. (2010) Structural basis for the specific inhibition of heterotrimeric Gq protein by a small molecule. *Proc. Natl. Acad. Sci. U.S.A.* **107,** 13666–13671
47. Grishina, G., and Berlot, C. H. (2000) A surface-exposed region of $G\alpha_s$ in which substitutions decrease receptor-mediated activation and increase receptor affinity. *Mol. Pharmacol.* **57,** 1081–1092
48. Zhang, Z., Melia, T. J., He, F., Yuan, C., McGough, A., Schmid, M. F., and Wensel, T. G. (2004) How a G protein binds a membrane. *J. Biol. Chem.* **279,** 33937–33945
49. Onrust, R., Herzmark, P., Chi, P., Garcia, P. D., Lichtarge, O., Kingsley, C., and Bourne, H. R. (1997) Receptor and $\beta\gamma$ binding sites in the α subunit of the retinal G protein transducin. *Science* **275,** 381–384
50. Lambright, D. G., Noel, J. P., Hamm, H. E., and Sigler, P. B. (1994) Structural determinants for activation of the α-subunit of a heterotrimeric G protein. *Nature* **369,** 621–628
51. Sondek, J., Lambright, D. G., Noel, J. P., Hamm, H. E., and Sigler, P. B. (1994) GTPase mechanism of G proteins from the 1.7-Å crystal structure of transducin α-GDP-AIF-4. *Nature* **372,** 276–279
52. Vetter, I. R., and Wittinghofer, A. (2001) The guanine nucleotide-binding switch in three dimensions. *Science* **294,** 1299–1304
53. Brugnera, E., Haney, L., Grimsley, C., Lu, M., Walk, S. F., Tosello-Trampont, A. C., Macara, I. G., Madhani, H., Fink, G. R., and Ravichandran, K. S. (2002) Unconventional Rac-GEF activity is mediated through the Dock180-ELMO complex. *Nat. Cell. Biol.* **4,** 574–582